Review J. Electrochem. Sci. Technol. 6(1), 7-15 (2015)

Journal of Electrochemical Science and Technology

Electrochemical Investigation of Inhibitory of New Synthesized 3-(4-Iodophenyl)-2-Imino-2,3-Dihydrobenzo[*d*]Oxazol-5-yl 4-Methylbenzenesulfonate on Corrosion of Stainless Steel in Acidic Medium

Ali Ehsani[1]*, Reza Moshrefi[2], and Maliheh Ahmadi[1]

[1]*Department of Chemistry, Faculty of Science, University of Qom, Qom, Iran*

[2]*Department of Chemistry, Faculty of Science, K. N. Toosi University of Technology, Tehran, Iran*

ABSTRACT

3-(4-Iodophenyl)-2-imino-2,3-dihydrobenzo[*d*]oxazol-5-yl 4-methylbenzenesulfonate (4-IPhOXTs) was synthesized and its inhibiting action on the corrosion of stainless steel 316L (SS) in sulfuric acid was investigated by means of potentiodynamic polarization and electrochemical impedance spectroscopy (EIS). The results of the investigation show that this compound has excellent inhibiting properties for SS corrosion in sulfuric acid. Inhibition efficiency increases with increase in the concentration of the inhibitor. The adsorption of 4-IPhOXTs onto the SS surface followed the Langmuir adsorption model with the free energy of adsorption ΔG^0_{ads} of -8.45 kJ mol^{-1}. Quantum chemical calculations were employed to give further insight into the mechanism of inhibition action of 4-IPhOXTs.

Keywords: Organic inhibitor, Adsorption, Stainless steel, Impedance, Density functional theory

Received May 2, 2014 : Revised August 22, 2014 : Accepted September 3, 2014

1. Introduction

Since iron and its alloys are the backbone of industrial constructions, many research projects have been concerned with their stability. One of most important tasks is the retardation of the attack by acid solutions used during pickling, industrial cleaning and descaling. The use of an additive is one of the major solutions for this problem. Hence, various additives are used to protect iron and its alloy against corrosive attack [1-5]. The use of organic molecules containing functional groups and p electrons in their structure, as corrosion inhibitors, is one of the most practical methods for protecting metals against corrosion and it is becoming increasingly popular. The existing data show that organic inhibitors act by adsorption and they protect the metal by film formation. Organic compounds bearing heteroatoms with high electron density such as phosphorus, sulfur, nitrogen, oxygen or those containing multiple bonds which are considered as adsorption centers, are effective as corrosion inhibitors [6-10]. The compounds containing both nitrogen and sulfur in their molecular structure have exhibited greater inhibition compared with those possessing only one of these atoms [11-13]. In the literature, many thiazole derivatives have been reported as

*Corresponding author. Tel.: (009825) 32103038

E-mail address: ehsani46847@yahoo.com & a.ehsani@qom.ac.ir(A. Ehsani)

Open Access DOI: http://dx.doi.org/10.5229/JECST.2015.6.1.15

corrosion inhibitors and found to have good corrosion inhibition effect [14,15]. The efficiency of an organic compound inhibitor is mainly dependent on its ability to adsorb on a metal surface, which consists of replacement of a water molecule at a corroding interface. In this study research methods including the weight loss method and electrochemical tests were employed to investigate the inhibition performance of new synthesized 4-IPhOXTs inhibitor in acidic solution. Quantum chemical calculations based on Density Functional Theory(DFT) method was performed on new compound used as corrosion inhibitor for SS in acid media to determine the optimized structural parameters, such as the frontier molecular orbital energy Highest occupied molecular orbital(HOMO) and Lowest unoccupied molecular orbital(LUMO).

2. Experimental

2.1 Materials and apparatus

Stainless steel 316L (SS) has the composition (wt %) Fe: 67.95, Ni: 10.60, Si: 0.45, Mn: 1.75, Cr: 16.50, S: 0.025, P: 0.028, Mo: 2.10, Al: 0.008, Co: 0.16, Cu: 0.35, Nb: 0.01 and V: 0.02. Surface of the working electrode was ground with silicon carbide abrasive paper from 400 to 1200, degreased with acetone, rinsed in distilled water, and dried in warm air. The corrosive medium was 0.5 M H_2SO_4 solution prepared from analytical reagent grade 98% sulfuric acid and distilled water. 3-(4-Iodophenyl)-2-imino-2,3-dihydrobenzo[*d*]oxazol-5-yl 4-methylbenzenesulfonate was synthesized in our laboratory from the reaction between 3-(4-iodophenyl)-2-imino-2,3-dihydrobenzo[*d*]oxazol-5-ol with *p*-toluenesulfonyl chloride and K_2CO_3 in EtOH under ultrasound irradiation for 2.5 h at room temperature [16]. The crude product was purified by aqueous ethanol [17,18] to afford the pure product (Yield 84%) and characterized by ^{1}H NMR, ^{13}C NMR, FT-IR, elemental analysis (CHN), and melting points. M.p. 199-201^{o}C; FT-IR (KBr, cm^{-1}): 3344, 3043, 1704, 1496, 1480, 1355, 1170, 1132, 1092, 893, 857, 819, 753, 592, 553; ^{1}H NMR (400 MHz, DMSO-d_6): δ_H = 7.89 (d, J = 8.4 Hz, 2H), 7.72 (d, J = 8.0 Hz, 2H), 7.36 (d, J = 8.0 Hz, 3H), 7.24 (d, J = 8.4 Hz, 2H), 7.09 (d, J = 8.8 Hz, 1H), 6.66 (d, J = 8.8 Hz, 1H), 6.58 (d, J = 2.4 Hz, 1H), 2.50 (s, 3H); ^{13}C NMR (100 MHz, DMSO-d_6): δ_C = 156.2, 145.7, 145.6, 142.9, 139.2, 133.7, 133.2, 131.9, 129.9, 128.7, 127.2, 116.0, 109.4, 103.6, 93.4, 21.8; CHN: Anal. Calcd for $C_{20}H_{15}IN_2O_4S$: C, 47.44; H, 2.99; N, 5.53. Found: C, 47.52; H, 3.10; N, 5.64.

The concentration range of 4-IPhOXTs employed was 1×10^{-4} to 10^{-3} M in 0.5 M sulfuric acid. All electrochemical measurements were carried out in a conventional three electrode cell, powered by a potentiostat/galvanostat (EG&G 273A) and a frequency response analyzer (EG&G, 1025). The system was run by a PC through M270 and M398 software via a GPIB interface. The frequency range of 100 kHz to 15 mHz and modulation amplitude of 5 mV were employed for impedance studies. A SS electrode was employed as the working electrode. A saturated calomel electrode (SCE) and a platinum wire were used as reference and counter electrodes, respectively. Before measurement, the working electrode was immersed in test solution for approximately 1 h until a steady open circuit potential (OCP) was reached. The polarization curves were carried out from cathodic potential of -1.4 V to anodic potential of 0.10 V with respect to the open circuit potential at a sweep rate of 0.5 mV/s. The linear Tafel segments of the anodic and cathodic curves were extrapolated to corrosion potential (E_{corr}) to obtain the corrosion current densities (i_{corr}). In each measurement, a fresh working electrode was used. For weight loss measurement, The SS sheets of 2.0×3.0×0.1 cm dimensions were abraded with different grades of sand papers, washed with distilled water, degreased with acetone, dried and kept in a desiccator. After weighing accurately by a digital balance with sensitivity of 0.1 mg the specimens were immersed in solution containing 0.5 M H_2SO_4 sol-u-tion with and without various concentrations of inhibitors. After 24 h exposure, the specimens were taken out rinsed thoroughly with distilled water, dried and weighted accurately again. Three parallel experiments were performed for each test. Several runs were performed for each measurement to obtain reproducible data.

2.2 Computational details

The use of quantum chemical calculations has become popular for screening new potential corrosion inhibitors [19]. Theoretical calculations were carried out at DFT level using the 6-31*G* (d,p) basis set for all atoms with Gaussian 03 program package. Electronic properties such as HOMO energy, LUMO energy and frontier molecular orbital coefficients have

been calculated. The molecular sketches of all compounds were drawn using Gauss View 03 [20].

3. Results and discussion

3.1 Potentiodynamic polarization studies

Polarization measurements were carried out to get information regarding the kinetics of anodic and cathodic reactions. The potentiodynamic polarization curves for SS in 0.5 M H_2SO_4 solution in the absence and presence of different concentrations of the inhibitor molecules are shown in Fig. 1. The values of electrochemical kinetic parameters such as corrosion potential (E_{corr}), corrosion current (I_{corr}) and Tafel slopes, determined from these by extrapolation method, are listed in Table 1. In corrosion, quantitative information on corrosion currents and corrosion potentials can be extracted from the slope of the curves, using the Stern-Geary equation, as follows [21]:

$$i_{corr} = \frac{1}{2.303R_p}\left(\frac{\beta_a \times \beta_c}{\beta_a + \beta_c}\right) \quad (1)$$

i_{corr} is the corrosion current density in A/cm^2; R_p is the corrosion resistance in ohms cm^2; β_a is the anodic Tafel slope in V/decade or mV/decade of current density; β_c is the cathodic Tafel slope in V/decade or mV/decade of current density; the quantity, $\beta_a \times \beta_c / \beta_a + \beta_c$, is referred to as the Tafel constant. The corrosion inhibition efficiency was calculated using the relation:

$$\eta(\%) = 100\left(\frac{i^*_{corr} - i_{corr}}{i^*_{corr}}\right) \quad (2)$$

where i^*_{corr} and i_{corr} are uninhibited and inhibited corrosion current densities, respectively, determined by extrapolation of Tafel lines in the corrosion potential. The corrosion rates η (mm/year) from polarization were calculated using the following Equation:

$$v = \frac{i_{corr} \times t \times M}{F \times S \times d} \times 10$$

where t is the time (s), M is the equivalent molar weight of working electrode (g/mol), F is Faraday constant (96500 C/mol), S is the surface area of electrode, d is the density of iron and the constant 10 is used to convert the unit cm to mm. The results are presented in Table 1. The inhibitor molecule first adsorbs on the SS surface and blocks the available reaction sites. As the concentration of the inhibitor increases, the linear polarization resistance (LPR) increases and corrosion

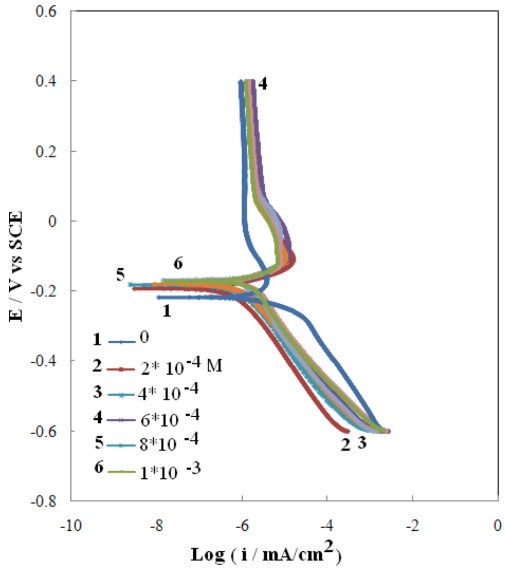

Fig. 1. Potentiodynamic polarization curves of SS in 0.5 M H_2SO_4 solution in the absence and presence of various concentrations of the 1,4-Ph(OX)$_2$(Ts)$_2$.

Table 1. Corrosion parameters obtained from Tafel polarisation curves of SS 316L in 0.5M H_2SO_4 in the absence and presence of different concentrations of 4-IPhOXTs at 298 K.

No.	Inhi. Con.	βa(v/decade)	βc(v/dedade)	I(μA)	E(V)	CR(mpy)
SS1	0	0.61	0.18	12.76	-0.22	5.25
SS2	0.0001	0.05	0.17	1.5	-0.19	0.62
SS3	0.0002	0.04	0.18	1.31	-0.16	0.57
SS4	0.0004	0.07	0.15	1.21	-0.18	0.50
SS5	0.0006	0.05	0.15	1	-0.18	0.40
SS6	0.0008	0.06	0.17	0.75	-0.16	0.3
SS7	0.001	0.05	0.16	0.66	-0.15	0.27

rate (CR) decreases. The surface coverage increases with the inhibitor concentration and the formation of inhibitor film on the SS surface reduces the active surface area available for the attack of the corrosive medium and delays hydrogen evolution and metal dissolution [22]. In the cathodic domain, as seen in Table 1, the values of âc show small changes with increasing inhibitor concentration, which indicates that the 4-IPhOXTs is adsorbed on the metal surface and the addition of the inhibitor hinders the acid attack on the SS electrode. In anodic domain, the value of âa decreases with the presence of 4-IPhOXTs. The shift in the anodic Tafel slope âa might be attributed to the modification of anodic dissolution process due to the inhibitor modules adsorption on the active sites. Compared to the absence of 4-IPhOXTs, the anodic curves of the working electrode in the acidic solution containing the 4-IPhOXTsclearly shifted to the direction of current reduction, as it could be observed from these polarization results; the inhibition efficiency increased with inhibitor concentration reaching a maximum value of 94.85% at 10^{-3} mol/L.

3.2 Electrochemical impedance spectroscopy

Electrochemical impedance spectroscopy is one of the best techniques for analyzing the properties of conducting polymer electrodes and charge transfer mechanism in the electrolyte/electrode interface. This has been broadly discussed in the literature using a variety of theoretical models [23-27]. Impedance measurements were performed under potentiostatic conditions after 1 h of immersion. Nyquist plots of uninhibited and inhibited solutions containing different concentrations of inhibitor molecules were performed over the frequency range from 100 kHz to 100 mHz and are shown in Fig. 2a and b. The similarity in the shapes of these graphs throughout the experiment indicates that the addition of inhibitor molecules does not cause any noticeable change in the corrosion mechanism [22]. The Nyquist diagrams show one capacitive loop at high frequencies. The capacitive loop at high frequencies represents the phenomenon associated with the electrical double layer. The above impedance diagrams (Nyquist) contain depressed semicircles with the center under the real axis. Such behavior is characteristic of solid electrodes and often referred to as frequency dispersion, attributed to different physical phenomena such as roughness, inhomogeneities of the solid surfaces, impurities, grain boundaries, and distribution of surface active sites. The ideal capacitive behavior is not observed in this case and hence a Constant Phase Element(CPE) is introduced in the circuit to give a more accurate fit [28-38]. Obviously, the corrosion behavior of SS in acidic solution is in influenced to some extent by mass transport since the Warburg impedance is observed in Nyquist plots. Anodic dissolution of SS dissolution is mass-transport limited and leads to the formation of sulfate compound. However, the diffusion step was ascribed either to sulfate ions transports to the surface or to the transport of formed compound diffusion to the bulk solution. The mechanism of corrosion remains unaffected during the addition of inhibitor molecules. The simplest equivalent circuit is represented in Fig. 2c, which is a parallel combination of the charge transfer

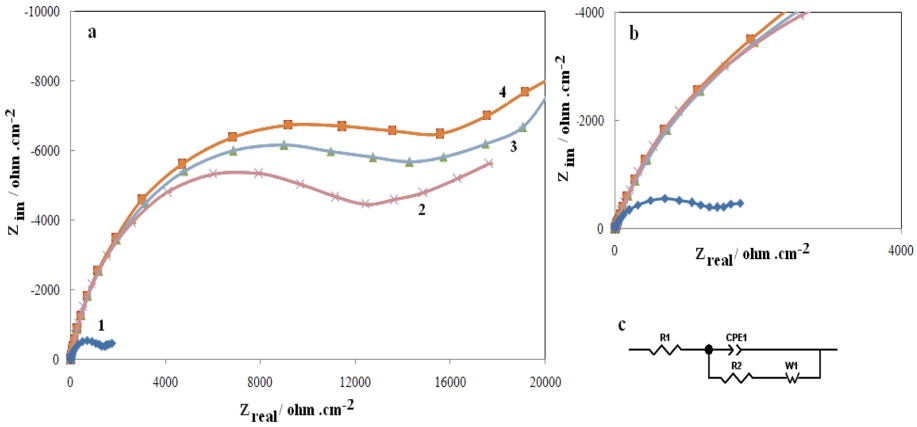

Fig. 2.(a, b) Nyquist plots of SS in 0.5 M H_2SO_4 solution containing different concentrations of the 1,4-Ph$(OX)_2(Ts)_2$ in different magnification . (c) Electrical equivalent circuit used for fitting.

resistance (R_{ct}) and CPE, both in series with the solution resistance (R_s). The impedance function of a CPE can be represented as:

$$Z_{CPE} = Y_0^{-1}(j\omega)^{-n} \quad (3)$$

where Y_0 is the CPE constant, ω is the angular frequency, and n is the CPE exponent, which can be used as a gauge of the heterogeneity or roughness of the surface [25,26]. W element in equivalent circuit presents Warburg impedance. In the present work, the value of n has a tendency to decrease with increasing inhibitor concentration, which may be attributed to the increase of inhibitor concentration resulted in the increasing surface roughness. For a circuit including a CPE, the double layer capacitance(C_{dl}) could be calculated from CPE parameter values Y_0 and n using the expression [22]:

$$C_{dl} = Y_0(\omega''_m)^{-n} \quad (4)$$

ω''_m is the frequency at which the imaginary part of the impedance has a maximum. As seen in Table 2, C_{dl} decreases with increase in concentration. This can be attributed to the gradual replacement of water molecules by the adsorption of the organic molecules at metal/solution interface, which is leading to a protective film on metal surface. In addition, the more the inhibitor is adsorbed, the more the thickness of the barrier layer increases according to the expression of the Helmholtz model [36]:

$$C_{dl} = \frac{\varepsilon\varepsilon_0 A}{d} \quad (5)$$

where d is the thickness of the protective layer, e is the dielectric constant of the medium, ε_0 is the vacuum permittivity and A is the surface area of the electrode. The equation used for calculating the percentage inhibition efficiency is:

$$\eta(\%) = 100\left(\frac{R^*_{ct} - R_{ct}}{R^*_{ct}}\right) \quad (6)$$

where R^*_{ct} and R_{ct} are values of the charge transfer resistance observed in the presence and absence of inhibitor molecules. Impedance parameters are summarized in Table 2. The results obtained from the EIS technique in acidic solution were in good agreement with those obtained from the polarization method. As observed in Table 2, the adsorption of 4-IPhOXTs molecules on SS surface modifies the interface between the corrosive medium and metal surface and decreases its electrical capacity. The increase in R_{ct} values with increase in 4-IPhOXTs concentration can be interpreted as the formation of an insulated adsorption layer. At the highest inhibitor concentration of 10^{-3} mol/L, the inhibition efficiency markedly increases and reaches 90.68%. Thus, it can be deduced that 4-IPhOXTs has a clear role in metal protection at the concentration of 10^{-3} M.

3.3 Weight loss measurements

At different temperatures (298-318 K), the results of weight loss measurements in 0.5 M H_2SO_4 solution without and with different concentrations of 4-IPhOXTs are shown in Table 3. The corrosion rate of SS was determined using the relation

$$W = \frac{\Delta m}{St} \quad (7)$$

where Δm is the mass loss, S the area and t is the immersion period. The inhibition efficiencies, $IE(\%)$, were calculated by the following equation:

Table 2. Impedance parameters for the corrosion of SS 316L in 0.5M H_2SO_4 containing different concentration of 4-IPhOXTsat 298 K

Concentration x (M)	Rs (Ω)	n	W (Ω)	P_{ct} (kΩ)	C_{dl} (μ Fcm^{-2})	IE%
0	4.25	0.91	1.45	1.85	31.91	
2.0×10^{-4}	7.42	0.87	1.42	14.81	24.46	87.50
4.0×10^{-4}	8.73	0.84	1.51	16.36	23.22	88.69
6.0×10^{-4}	8.85	0.83	1.35	17.25	21.15	89.27
8.0×10^{-4}	9.17	0.83	1.29	18.24	20.54	89.85
1.0×10^{-3}	9.75	0.81	1.38	19.85	20.14	90.68

Table 3. Results of weight loss test and IE_w% of 1, 4-Ph $(OX)_2(Ts)_2$ inhibitor with different concentration and different temperature in 0.5 M H_2SO_4

Inhibitor concentration (M)	Corrosion rate ($mg/cm^2/h$) (298K)	IE_w %	Corrosion rate ($mg/cm^2/h$) (308K)	IE_w%	Corrosion rate ($mg/cm^2/h$) (318K)	IE_w%
0	5.16		7.87		10.12	
2.0×10^{-4}	0.85	83.52	1.42	81.95	1.94	80.83
4.0×10^{-4}	0.72	86.04	1.22	84.49	1.69	83.30
6.0×10^{-4}	0.65	87.43	1.11	85.89	1.49	85.27
8.0×10^{-4}	0.51	90.01	0.92	88.31	1.26	87.54
1.0×10^{-3}	0.46	91.08	0.85	89.19	1.15	88.63

$$IE(\%) = \left(\frac{W_0 - W}{W_0}\right) \times 100 \quad (8)$$

W_0 and W are the corrosion rates in the absence and presence of the inhibitors, respectively. From Table 3, it can be found that as temperature increases, the corrosion rate improves and *IE*(%) reduces. This phenomenon might be attributed to the fact that higher temperature could speed up hot movement of the organic molecules and weaken the adsorption ability of inhibitor on metal surface. It can also be seen in Table 3 that the increase in inhibitor concentration leads to an increase in inhibition efficiency and a decrease in corrosion rate. This result suggests that plenty of adsorbed inhibitor molecules move onto the metal surface. Then, the contact area between metal surface and aggressive solution becomes smaller and smaller leading to the decrease in active sites. The inhibition efficiency obtained by weight loss measurements is lower than that from electrochemical experiments. This difference is attributed to weight loss experiments giving average corrosion rates, whereas the electrochemical experiments give instantaneous corrosion rates. Therefore, the discrepancy in inhibition efficiency obtained by the two methods is understandable. However, the trend in inhibition efficiency with increasing inhibitor concentration is similar regardless of the selection of electrochemical or weight loss method. The inhibition efficiency increases as inhibitor concentration increases.

3.4 Adsorption isotherms

The adsorption of an organic adsorbate at metal/solution interface can be presented as a substitution adsorption process between the organic molecules in aqueous solution, (Org_{aq}), and the water molecules on metallic surface, (H_2O_{ads}) Org_{aq}

$$Org_{aq} + XH_2O_{ads} \leftrightarrow Org_{ads} + XH_2O_{aq} \quad (9)$$

where X, the size ratio, is the number of water molecules displaced by one molecule of organic inhibitor. X is assumed to be independent of coverage or charge on the electrode [37]. Basic information on the interaction between the inhibitors and the steel surface is provided by the adsorption isotherm. The degree of surface coverage, θ, at different inhibitor concentrations in 0.5 M H_2SO_4 was evaluated from weight loss measurements (θ= IE(%)/100) at 25°C. The plot of C/θ against inhibitor concentration, C, displayed a straight line for the tested inhibitor (Fig. 3). The linear plot clearly revealed that the surface adsorption process of 4-IPhOXTs on the SS surface obeys the Langmuir isotherm. Likewise, it suggests that an adsorption process occurs, which can be expressed as follows [38]:

$$\frac{C}{\theta} = \frac{1}{K_{ads}} + C \quad (10)$$

where K_{ads} is the equilibrium constant of the adsorp-

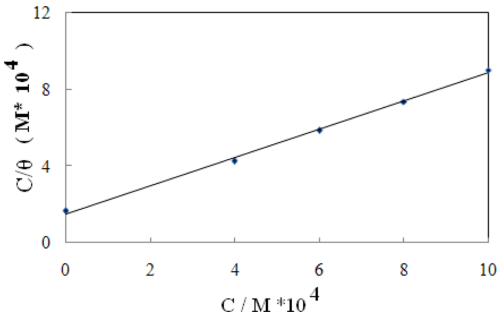

Fig. 3. Langmuir adsorption plot for SS in 0.5 M H_2SO_4 containing different concentrations of 1,4-Ph$(OX)_2(Ts)_2$.

tion process. Free energy of adsorption (ΔG_{ads}) can be calculated by Eq. (11). The numeral of 55.5 is the molar concentration of water in the solution:

$$K_{ads} = \frac{1}{55.5}\exp\left(\frac{-\Delta G^{0}_{ads}}{RT}\right) \quad (11)$$

The value of ΔG^0 ads for adsorption of 4-IPhOXTs was found to be -8.45kJ mol^{-1}. The negative value of ΔG^0 ads suggests that 4-IPhOXTsis spontaneously adsorbed on the SS surface. Literature survey reveals that the values of ΔG^0_{ads} around -20 kJ mol^{-1} or lower are consistent with the electrostatic interaction between the charged molecules and the charged metal (physical adsorption) [39]. The adsorption of an inhibitor on the metal surface can occur on the basis of donor-acceptor interactions between the p-electrons of the heterocyclic compound and the vacant d-orbitals of the metal surface atoms. Therefore, the energies of the frontier orbitals should be considered. Energy of LUMO shows the ability of the molecule to receive charge when attacked by electron pair donors, even as the energy of HOMO to donate the charge when attached by electron seeking reagents. As the energy gap between the frontier orbitals gets smaller, the interactions between the reacting species strengthen [40]. In this regard, the electronic properties such as HOMO energy, LUMO energy and frontier molecular orbital coefficients have been calculated for prepared inhibitor. Results are presented in Fig. 4 and Tables 4. According to the results, HOMO location in the 4-IPhOXTs molecule is mostly distributed in the vicinity of the nitrogen, oxygen atoms. This indicates the reactive sites of the interaction between 4-IPhOXTs and the SS surface. Mulliken population analysis, presented in Fig. 4e, is further evidence for the interaction between SS surface and inhibitor active sites. It is clear from figure 4 that the nitrogen atoms of 4-IPhOXTs have considerable excess of negative charge than other atoms. Thus, the adsorption of 4-IPhOXTs as a neutral mole-

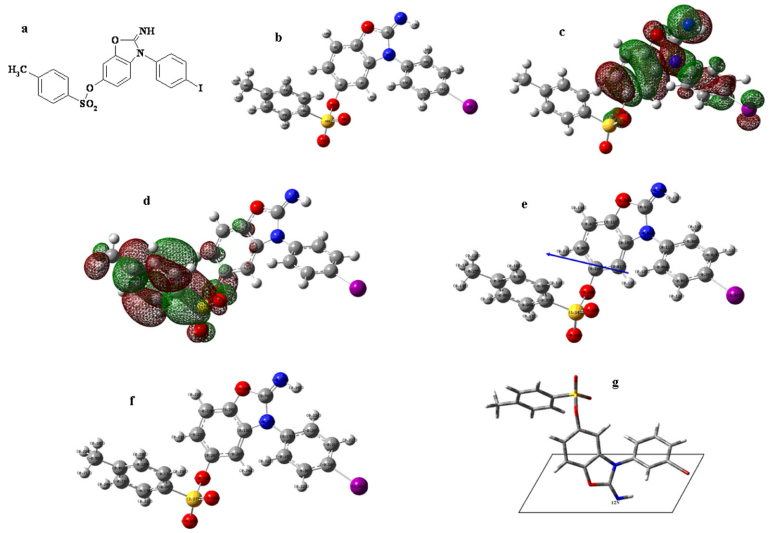

Fig. 4. (a) Structure of 1,4-Ph$(OX)_2(Ts)_2$; (b) Optimized molecular structure of 1,4-Ph$(OX)_2(Ts)_2$, H atoms have been omitted for clarity; (c) HOMO of 1,4-Ph$(OX)_2(Ts)_2$; (d) LUMO of 1,4-Ph$(OX)_2(Ts)_2$; (e) Muliken charge population analysis and vector of dipole moment of 1,4-Ph$(OX)_2(Ts)_2$; (f) Natural charge population analysis of 4-IPhOXTs and (g) The schematic representation of the adsorption behavior of 4-IPhOXTs on the surface of the SS.

Table 4. Orbital energies for HOMO, LUMO, HOMO-LUMO gap energy (E) and dipole moment (μ) of 4-IPhOXTs in the gaseous (G) and aqueous (A) phases*.

Phase	E_{HOMO}(ev)	E_{LUMO}(ev)	E(ev)	μ(D)
G	-5.533	-1.321	4.212	8.7507
A	-5.532	-1.322	4.210	8.7512

*All quantum chemical parameters calculated at DFT level using the 6-31G(d,p) basis set.

cule on the metal surface can occur directly involving the displacement of water molecules from the metal surface and sharing of electrons between the nitrogen atoms and the metal surface. It should be noted that 4-IPhOXTs adsorbs mainly through electrostatic interactions between the positively charged nitrogen atom (since acidic solution can protonate the nitrogen atoms of 4-IPhOXTs and the negatively charged metal surface (physisorption) as evident in the value of ΔG^0_{ads} obtained.

4. Conclusion

4-IPhOXTs was found to inhibit the corrosion of SS in 0.5 M H_2SO_4 solution and the extent of inhibition was concentration dependent. Inhibition efficiency increases with increasing inhibitor concentration. EIS plots indicate that the charge transfer resistances increase with increasing concentration of the inhibitor at the highest inhibitor concentration of 10^{-3} M, the inhibition efficiency increases. 4-IPhOXTs inhibits corrosion by getting adsorbed on the metal surface following Langmuir adsorption isotherm. Quantum chemical calculations show that the adsorption sites are mainly located around the nitrogen atoms of 4-IPhOXTs.

Acknowledgements

We gratefully acknowledge the support of this work by Qom University Research Council.

References

[1] I. Ahamad, M.A. Quraishi, Corros. Sci. 51 (2009) 2006-2013.
[2] Q.B. Zhang, Y.X. Hua, Electrochim. Acta 54 (2009) 1881-1887.
[3] W. Li, Q. He, C. Pei, B. Hou, Electrochim. Acta 52 (2007) 6386-6394.
[4] R. Solmaz, G. Kardas, B. Yazýcý, M. Erbil, Prot. Met. 41 (2005) 581-585.
[5] G. Kardas, Mater. Sci. 41 (2005) 337-343.
[6] J. Aljourani, K. Raeissi, M.A. Golozar, Corros. Sci. 51 (2009) 1836-1843.
[7] M.L. Zheludkevich, K.A. Yasakau, S.K. Poznyak, M.G.S. Ferreira, Corros. Sci. 47 (2005) 3368-3383.
[8] I.B. Obot, N.O. Obi-Egbedi, S.A. Umoren, Corros. Sci. 51 (2009) 276-282.
[9] M.G. Hosseini, M. Ehteshamzadeh, T. Shahrabi, Electrochim. Acta 52 (2007) 3680-3685.
[10] S. S. Afak, B, Duran, A. Yurt, G. Turkoglu, Corros. Sci. 54 (2012) 251-259.
[11] H.H. Hassan, E. Adbelghani, M.A. Amin, Electrochim. Acta 52 (2007) 6359-6366.
[12] Y. Abdoud, A. Abourrriche, T. Saffaj, M. Berrada, M. Charrouf, A. Bennamara, N. Al Himidi, H. Hannache, Mater. Chem. Phys. 105 (2007) 1-5.
[13] M.A. Quaraishi, J. Rawat, M. Ajmal, J. Appl. Electrochem. 30 (2000) 745-751.
[14] K.F. Khaled, M.A. Amin, Corros. Sci. 51 (2009) 1964-1975.
[15] I.B. Obot, N.O. Obi-Egbedi, Corros. Sci. 52 (2010) 282-285.
[16] D. Habibi, M. Nasrollahzadeh, H. Sahebekhtiari, R.V. Parish, Tetrahedron, 69 (2013), 3082-3087.
[17] D. Habibi, M. Nasrollahzadeh, Y. Bayat. Synth. Commun, 41(2011) 2304-2308.
[18] D. Habibi, M. Nasrollahzadeh. Synth. Commun, 42(2012) 2023-2032
[19] A. Kokalj, Electrochim. Acta 56 (2010) 745-755.
[20] Gauss View, Version 3.0, Gaussian Inc., Pittsburgh, PA, 2003.
[21] M.G. Mahjani, R. Moshrefi, A. Ehsani, M. Jafarian, Anti-Corros. Methods Mater, 58 (2011) 250-257.
[22] T. Zhihua, Z. Shengtao, L. Weihua, H. Baorong, Ind. Eng. Chem. Res 50 (2011) 6082-6088.
[23] A. Ehsani, M.G. Mahjani, M. Jafarian, Turk. J. Chem. 35 (2011) 1-9.
[24] A. Ehsani, F. Babaei, M. Nasrollahzadeh, Appl. Surf. Sci. 283 (2013) 1060-1064.
[25] A. Ehsani, M. G. Mahjani, M. Jafarian, A. Naeemy, Electrochim. Acta 71 (2012) 128-133.
[26] A. Ehsani, M.G. Mahjani,M. Jafarian, A. Naeemy, Prog. Org. Coat. 69 (2010) 510-516.
[27] A. Ehsani, M.G. Mahjani, M. Jafarian, Synth. Met. 161 (2011) 1760-1765.
[28] A. Ehsani, M.G. Mahjani, M. Bordbar, S. Adeli, J. Electroanal. Chem. 710 (2013) 29-35.
[29] A. Ehsani, M G. Mahjani, R. Moshrefi, H. Mostaanzadeh, J. Shabani, RSC. Adv. 4 (38) (2014), 20031 - 20037.
[30] A. Ehsani, M. Nasrollahzadeh, MG. Mahjani, R. Moshrefi, H. Mostaanzadeh, Ind. Eng. Chem. 20 (2014) 4363-4370.
[31] A. Ehsani, M.G. Mahjani, M. Nasseri, M. Jafarian. Anti-Corros. Methods Mater, 61 (2014) 146-152.
[32] A. Ehsani, N. Ajami, F. Babaei, H. Mostaanzadeh, Synth. Met. 197 (2014)80-85.
[33] A. Ehsani, M.G. Mahjani, S. Adeli, S. Moradkhani, Prog. Org. Coat. 77 (2014) 1674-1681.
[34] A. Ehsani, S. Adeli, F. Babaei, H. Mostaanzadeh, M. Nasrollahzadeh, J. Electroanal. Chem. 713 (2014) 91.
[35] M.G. Mahjani, R. Moshrefi, A. Ehsani, M. Jafarian, Anti-Corros. Methods Mater. 58 (2011) 250-257.
[36] Hassan, H. Electrochim. Acta 51 (2006) 5966-5972.
[37] S. Martinez, Mater. Chem. Phys. 77 (2002) 97-102.
[38] P. Hohenberg, W. Kohn, Phys. Rev. A136 (1964) 864.

[39] I.B. Obot, N.O. Obi-Egbedi, S.A. Umoren, Corros. Sci. 51 (2009) 1869.
[40] M. Ozcan, F. Karadag, I. Dehri, Acta Phys. Chim. Sin. 24 (8) (2008) 1387.

Table 5. Electronegativity (÷), global hardness (ç) and proportion of electrons transferred (N) of 1,4-$Ph(OX)_2(Ts)_2$.

Table 6. Muliken and Natural Charges (e) for atoms in 1,4-$Ph(OX)_2(Ts)_2$.